Title
A MODULATED MOLECULAR BEAM STUDY OF THE ENERGY OF SIMPLE GASES SCATTERED FROM PYROLYTIC GRAPHITE

Author
Siekhaus, W.J.

Publication Date
1972-05-01

Submitted to Surface Science

LBL-843
Preprint

A MODULATED MOLECULAR BEAM STUDY OF THE ENERGY OF SIMPLE GASES SCATTERED FROM PYROLYTIC GRAPHITE

W. J. Siekhaus, J. A. Schwarz, and D. R. Olander

May 1972

AEC Contract No. W-7405-eng-48

LBL-843

DISCLAIMER

A MODULATED MOLECULAR BEAM STUDY OF THE ENERGY OF SIMPLE GASES SCATTERED FROM PYROLYTIC GRAPHITE

by

W.J. Siekhaus, J.A. Schwarz, and D.R. Olander

Inorganic Materials Research Division of the
Lawrence Berkeley Laboratory
and
Department of Nuclear Engineering
University of California, Berkeley, California 94720

ABSTRACT

The energy of rare gases and several diatomic gases after scattering from pyrolytic graphite was determined by molecular beam-phase sensitive detection methods. The angle of incidence of the molecular beam and the angle of sampling of the reflected molecules were both fixed at 45°. The phase shifts induced by changing either the temperature of the incident gas or the solid were utilized to determine the temperature of the scattered molecules.

The results showed that the temperature of the reflected molecules was independent of the temperature of the incident gas. With increasing solid temperature, the reflected gas temperature increased up to a limiting value which was dependent on the gas and the surface only. Both the basal and prismatic faces of graphite were investigated. In addition, a prism plane specimen which had not been subjected to high temperature heat treatment was studied. The temperature of the reflected beam did not depend upon the crystallographic face of the graphite but was markedly reduced by high temperature annealing.

INTRODUCTION

Classical and quantum mechanical treatments dealing with the thermal accomodation of gases with solid surfaces have been presented for over thirty five years (1-5). Only recently, however, has the effect of solid temperature been explicitly treated in theoretical models. The Trilling (6) model assumes that the solid is a semi-infinite elastic continuum and postulates the existence of a "Knudsen layer" near the surface which serves to modify the incident gas distribution function, $f_o(v')$, to produce a distribution function of the reflected gas, $f(v)$. When the energy of the incident gas molecule is less than the well depth of the gas-solid interaction potential, Trilling's calculation predicts how the thermal accomodation coefficient depends upon the ratio of the surface temperature and the gas temperature. When the incident energy of the gas is greater than the well depth, the ac should be independent of surface temperature. This theory places no restriction on the masses of the solid and gas atoms. Trilling found satisfactory agreement between theory and the experimental results for rare gases on tungsten reported by Thomas and Menzel (7). Forman (8) has applied the soft cube model with a simplified interaction potential to calculate the average speed of atoms rebounding from a surface. Computations were performed for monoenergetic beams of krypton incident upon a tungsten surface.

The only energy exchange measurements on

graphite are those of Meyer and Gomer (9). Their study of thermal accomodation of rare gases on graphite filaments suggested that the gas atoms were released from the surface at a critical temperature which was proportional to the binding energy of the gas on graphite.

In the present experiment, the mean energy of simple gases scattered from pyrolytic graphite was measured. Both the temperature of the solid and of the incident beam were varied independently.

EXPERIMENTAL

The artificial form of graphite known as pyrolytic graphite was employed in the present work, primarily because it is much denser and of higher purity than ordinary graphite and because it can be fabricated so as to expose either the basal or prismatic surfaces to the incident gas beam. These two surfaces exhibit remarkably different chemical behavior with respect to oxygen (10).

In addition to studying the effect of crystallographic orientation of the surface by utilizing basal and prism faces, the effect of heat treatment upon thermal accomodation was investigated. Pyrolytic graphite is produced at temperatures of $\sim$2000°C. This product is only $\sim$96% of theoretical density. Heat treatment at $\sim$3000°C increases the density to >99% of the theoretical value by increasing the perfection of the bulk

crystallites. Such heat treatment might also affect surface properties. We have conducted tests upon the pyrolytic graphite in the prism plane orientation both in the "as-received" and in the "annealed" condition. The basal plane specimen was annealed.

All samples were prepared for the experiment by polishing to a high luster with diamond paste followed by extended heating (at $\geq$1500°C) under high vacuum in the apparatus. All gases were research grade purity. Except for xenon, they were passed through a liquid nitrogen cold trap before use.

The energy measurements were performed with the modulated molecular beam technique. In this method, a modulated beam of gas atoms or molecules impinges upon a target located in a high vacuum environment (background pressure $\sim 10^{-8}$ torr, equivalent beam pressure $\sim 10^{-4}$ torr). The interaction may be chemical and produce a species different from the incident gas. Or, the interaction may be purely physical and merely change a property of the incident gas (such as its direction or energy). Application of this method to chemical interactions of oxygen beams with pyrolytic graphite is reported elsewhere (10).

Inasmuch as phase-lock detection is employed in such experiments, non-chemical interactions may be observed by the effect of beam and solid temperatures on the amplitude and phase angle of the reflected beam signal. These two quantities are affected by molecular flight times in the apparatus, which in turn depend upon the mean speeds of the molecules as they travel from the beam modulator to the solid

surface and from the solid surface to the detector. If the molecular velocity distribution in both legs of the total flight path is assumed to be Maxwellian, the mean speeds may be interpreted in terms of corresponding temperatures. Holister et al (11) were the first to apply phase-lock detection to thermal accomodation measurements (they studied hydrogen on copper). Yamamoto and Stickney (12) have utilized transit phase shifts to measure the mean speed of monoenergetic argon beams scattered from tungsten.

A schematic of the apparatus is shown in Fig. 1. The incident beam travels 2.8 cm from the location at which it is symmetrically modulated by a rotating toothed disk to the solid target. The molecules reflected from the target enter the mass spectrometer detector after traversing a flight path of 4.2 cm. The angles of beam incidence and sampling are both 45° and cannot be varied. A detailed description of the apparatus is given elsewhere (13).

THEORY OF THE METHOD

As described in ref 13, the output from the detector is compared to a reference signal generated by the beam modulator in a lock-in amplifier. This instrument provides a measure of the amplitude and the phase angle of the output signal. Although both of these quantities depend upon the temperatures of the incident and the reflected beams, only the phase information was utilized in the present work. The phase is affected by fewer experimental variables than is the amplitude. The latter, for example, may vary because of drift of the gains of the electronic signal processing equipment, but the phase does not. The amplitude is dependent upon the angular distribution of the reflected molecules which may change with beam or solid temp-

erature. The phase lag, on the other hand, is not affected by this phenomenon.

The transit phase lag is defined as the difference between the phase angle of the output signal when the molecular beam is modulated at a frequency ω and the phase angle of the signal as the chopping frequency approaches zero. Because the mass spectrometer detector used in the present study is a density-sensitive device, the response of the lock-in amplifier is determined by the periodic variation of the number density of scattered beam molecules in the ionizer. This quantity may be calculated as follows.

Consider a steady (unmodulated) molecular beam of intensity I_o striking the target. Let $I_o(v')$ be the speed distribution in the beam, so that:

$$I_o = \int_0^\infty I_o(v')\,dv' \tag{1}$$

$I_o(v')$ may also be written as:

$$I_o(v') = v' n_o f_o(v') \tag{2}$$

where n_o is the total number density in the beam as it strikes the target and $f_o(v')$ is the distribution function of the number density of the incident beam. If the beam is Maxwellian,

$$f_o(v') = \frac{4}{\sqrt{\pi}} \frac{(v')^2}{v_m^3} e^{-(v'/v_m)^2} \tag{3}$$

where $v_m = (2kT_B/m)^{1/2}$ is the most probable speed. T_B is the temperature of the source generating the primary beam and m is the molecular mass.

If the molecular beam is now modulated before striking the target, the intensity distribution may be written as:

$$I_o(v',t) = I_o(v')g(t-\ell_1/v') \tag{4}$$

where g(t) is the gating function of the chopper. It represents the fraction of the beam cross sectional area which is open at time t. Eq(4) states that the intensity of the portion of the modulated beam in the speed range v' to v'+dv' is reduced from the steady state value by the fraction of the beam passed by the chopper at a time ℓ_1/v' prior to the time t. ℓ_1 is the distance between the chopper and the target and ℓ_1/v' is the transit time on this path for a molecule of speed v'.

Assuming that the time spent by a molecule on the solid surface before re-emission is small compared to the transit time, the rate at which molecules with speeds in the range v to v+dv leave the surface in the solid angle subtended by the detector is given by:

$$R_E(v,t) = A_B P_\theta \int_0^\infty I_o(v',t)p(v',v)dv' \tag{5}$$

where A_B is the cross sectional area of the beam striking the target and P_θ is the fraction of the molecules striking the surface which are reflected into the solid angle subtended by

the detector. The second quantity in the integrand of Eq(5) is the scattered speed transfer function for the particular combination of incidence and scattering angles utilized. $p(v',v)dv$ is the probability that a molecule of speed v' impinging upon the solid is scattered into the solid angle of the detector with a speed after collision between v and $v+dv$ (14).

The number density distribution of reflected molecules in the detector at time t is given by:

$$n_D(v,t) = \beta R_E(v,t-\ell_2/v)/v \qquad (6)$$

where ℓ_2 is the distance between the solid surface and the detector and β is a geometrical factor equal to the solid angle subtended by the detector divided by the square of the surface-to-detector distance. Inserting Eqs(2), (4), and (5) into (6) and integrating over all speeds of the reflected molecules yields the total number density in the ionizer.

$$n_D(t) = \beta A_B P_\theta n_o \int_0^\infty \frac{dv}{v} \int_0^\infty dv' v' f_o(v') p(v',v) g(t - \frac{\ell_1}{v'} - \frac{\ell_2}{v}) \qquad (7)$$

The physics of the gas-solid interaction is contained in the transfer function $p(v',v)$. For example, if scattering is specular and elastic, $p(v',v) = \delta(v-v')$. Another case, and the one utilized in the present investigation, occurs if the incident molecules are trapped on the surface long enough so that they forget their initial speeds. The trapping time is assumed

to be small compared to the flight time. The momentarily trapped molecule need not acquire sufficient energy to equilibrate thermally with the solid, in which case thermal accomodation would be complete. In the case of such a "memoryless" collision, the scattering transfer function is independent of the incident speed v'. It may be shown that for this case, p(v) is related to the number density speed distribution of the scattered molecules by:

$$p(v) = vf(v)/\bar{v} \tag{8}$$

where $\bar{v}$ is the mean speed of the reflected molecules:

$$\bar{v} = \int_0^\infty vf(v)\,dv \tag{9}$$

f(v) need not be Maxwellian. However, since our experiment permits us to determine only one parameter characterizing the reflected beam we assume that f(v) is Maxwellian at a temperature T_R. If $T_R = T_s$ (the solid temperature), then thermal accomodation is complete.

Substituting Eq(8) into Eq(7) yields:

$$n_D(t) = \beta A_B P_\theta n_o \frac{\bar{v}_o}{\bar{v}} \int_0^\infty f(v) \left\{ \frac{1}{\bar{v}_o} \int_0^\infty v' f_o(v') g(t-\ell_1/v' - \ell_2/v)\,dv' \right\} dv \tag{10}$$

where $\bar{v}_o$ is the mean speed of the incident beam.

To determine the phase lag of the signal, $n_D(t)$ is expanded

in a Fourier series. Since only the first Fourier coefficients are of interest (the lock-in amplifier is set to respond only to the fundamental mode of the signal it receives), the gating function for use in Eq(10) may be written as:

$$g(t) = g_o e^{i\omega t} \tag{11}$$

where ω is the modulation frequency and g_o is the coefficient of the fundamental mode of the gating function. Similarly, $n_D(t)$ may be expanded in a Fourier series and only the first term retained:

$$n_D(t) = \bar{n}_D e^{i\omega t} \tag{12}$$

The quantity $\bar{n}_D$ is the coefficient of the fundamental mode of $n_D(t)$. In general, it is a complex quantity because the density in the detector lags behind the gating function as a result of the time that the molecules spend in flight. If Eqs(11) and (12) are substituted into Eq(10), there results:

$$\frac{\bar{n}_D}{\bar{n}_{Do}} = \left\{ \int_0^\infty e^{-i\omega \ell_2/v} f(v)\,dv \right\} \left\{ \frac{1}{\bar{v}_o} \int_0^\infty v' e^{-i\omega \ell_1/v'} f_o(v')\,dv' \right\} \tag{13}$$

where

$$\bar{n}_{Do} = \beta A_B n_o \frac{\bar{v}_o}{\bar{v}} g_o \tag{14}$$

is the value attained by $\bar{n}_D$ as $\omega \to 0$.

By writing $e^{-ix} = \cos x - i\sin x$, Eq(13) may be expressed by:

$$\frac{\bar{n}_D}{\bar{n}_{Do}} = \left[I_f(X_1)I_d(X_2) - K_f(X_1)K_d(X_2)\right] - i\left[K_f(X_1)I_d(X_2)+I_f(X_1)K_d(X_2)\right] \tag{15}$$

where

$$X_1 = \omega\ell_1 \sqrt{m/2kT_B} \tag{16}$$

$$X_2 = \omega\ell_2 \sqrt{m/2kT_R} \tag{17}$$

and the functions I_f, I_d, K_f and K_d are given by:

$$I_d(X) = \int_0^\infty f(y)\cos(X/y)\,dy \tag{18}$$

$$I_f(X) = \frac{\sqrt{\pi}}{2}\int_0^\infty yf(y)\cos(X/y)\,dy \tag{19}$$

$$K_d(X) = \int_0^\infty f(y)\sin(X/y)\,dy \tag{20}$$

$$K_f(X) = \frac{\sqrt{\pi}}{2}\int_0^\infty yf(y)\sin(X/y)\,dy \tag{21}$$

These functions have been tabulated by Harrison et al (15).

The transit phase lag is the polar angle of the complex quantity on the right hand side of Eq(13):

$$\tan\phi = \frac{K_f(X_1)I_d(X_2) + I_f(X_1)K_d(X_2)}{I_f(X_1)I_d(X_2) - K_f(X_1)K_d(X_2)} \tag{22}$$

which may also be written as:

$$\phi = \phi_f(X_1) + \phi_d(X_2) \tag{23}$$

where

$$\tan \phi_f(X_1) = K_f(X_1)/I_f(X_1) \tag{24}$$

$$\tan \phi_d(X_2) = K_d(X_2)/I_d(X_2) \tag{25}$$

The functions $\phi_f(X)$ and $\phi_d(X)$ are plotted in Fig. 2.

For the memoryless collision, the transit phase lag is the sum of the phase lag of the flux for the path from the chopper to the surface and the phase lag of the number density for the leg from the surface to the detector. For molecules with a distribution of incident velocities, the separability of the transit phase lag implied by Eq(23) is valid only if the velocity distribution of the reflected beam is independent of incident velocity. Yamamoto and Stickney (16) termed this type of interaction an "uncorrelated Maxwellian". They found (unnecessarily, we believe) that the transit phase lag required numerical solution rather than the simple analytic formula Eq(23).

For the case of specular reflection (i.e., no energy exchange), $p(v',v) = \delta(v'-v)$ and the transit phase lag is:

$$\tan \phi = K_d(X_T)/I_d(X_T) \tag{26}$$

where:

$$K_T = \omega(\ell_1+\ell_2)\sqrt{m/2kT_B} \qquad (27)$$

Eqs(26) and (27) show that in the elastic collison limit, the phase lag is due simply to transit of the incident beam over the entire flight path. The solid surface serves only to change the direction of the beam.

Yamamoto and Stickney (16) have considered a primitive type of "correlated Maxwellian" transfer function described by $p(v',v) = \delta(v-(T_R/T_B)^{1/2}v')$, for which the transit phase lag is given by Eq(26) with:

$$X_T = \omega[\ell_1 + (T_B/T_R)^{1/2}\ell_2]\sqrt{m/2kT_B}$$

The method of analyzing the data thus depends upon prior specification of the form of the velocity transfer function. The experiment does not provide enough information to determine the complete function $p(v',v)$. Each measured transit phase lag can be utilized to determine a single parameter which characterizes the gas-solid energy exchange. In the memoryless collision case, the parameter is the temperature of the reflected molecules. There is no adjustable parameter in the specular scattering case. However, if partial energy accomodation is regarded as specular reflection of a fraction of the incident molecules and complete accomodation of the remainder, a parameter which may be determined from the data is introduced. We have not used this method of data interpretation.

Inasmuch as the analysis of the energy exchange process depends heavily upon the validity of Eq(23), it was important to verify its accuracy for a situation in which the reflected beam temperature was assumed to be known. To this end, beams of inert gases at room temperature (300°K) were scattered from the graphite also at 300°K. The phase shifts were measured as a function of modulation frequency. Unwanted phase shifts associated with the apparatus and signal processing (13) were removed from the measured phase angles. If the temperature of the reflected beam is assumed to be 300°K as well, and the speed distributions of the incident and reflected beams are assumed to be Maxwellian (17), the phase lag may be calculated from Eqs(16), (17), and (23) and Fig. 2. Fig. 3 shows the excellent agreement of theory with experiments on both surfaces of graphite. We therefore may place confidence in the accuracy of the phase shifts which are measured when the beam and/or the solid is heated. The test does not, however, demonstrate that the particular type of speed transfer function used to derive Eq(23) is valid when the beam and the solid are at different temperatures. Although the modulation frequency was used as the variable in the test with room temperature beams and solid, a constant chopping frequency of 1500 Hz was used for all experiments in which the gas and solid temperatures were varied.

Since phase shifts can be measured with much greater accuracy than absolute phase angles, the following method was utilized to determine the transit phase lag. First, with the

beam at 300°K, the phase shift $\Delta\phi_{(\text{target heat})}$ due to heating of the target from 300°K to T_s was measured. Second, with the target temperature held constant at T_s, the phase shift $\Delta\phi_{(\text{beam heat})}$ accompanying increase of beam temperature from 300°K to T_B was measured. If the measured phase angle for a particular combination of beam and solid temperatures is denoted by $\phi(T_s,T_B)$, the total phase shift in going from a "cold" condition (T_s=300°K, T_B=300°K) to a "hot" condition may be expressed by:

$$\phi(T_s,T_B) - \phi(300,300) = [\phi(T_s,T_B)-\phi(T_s,300)]+[\phi(T_s,300)-\phi(300,300)]$$

$$= -\Delta\phi_{(\text{beam heat})} - \Delta\phi_{(\text{target heat})} \qquad (28)$$

where the phase shifts due to beam and target heating are defined so as to be positive quantities (the phase angle under hot conditions is less than that with the system cold). For a given molecular species and a specified modulation frequency, Eqs(16) and (17) show that the characteristic transit phase lags ϕ_f and ϕ_d are functions of T_B and T_R only. Using Eq(23), the left hand side of Eq(28) may be expressed by:

$$\phi(T_s,T_B)-\phi(300,300) = [\phi_f(T_B)+\phi_d(T_R)]-[\phi_f(300)+\phi_d(300)] \qquad (29)$$

Equating the right hand sides of the two preceding equations yields:

$$\phi_d(T_R) = \phi_d(300) - \Delta\phi_{(\text{target heat})} - \Delta\phi_{(\text{beam heat})} + [\phi_f(300) - \phi_f(T_B)] \quad (30)$$

The first and fourth terms on the right hand side of Eq(30) are computed by using Fig 2 and the temperature indicated as the arguments in the X values for the appropriate flight paths. The accuracy of these theoretically deduced terms has been verified by the room temperature test described earlier. The phase angle of the reflected beam, $\phi_d(T_R)$ is determined from the measured phase shifts due to beam and target heating and Eq(30). The temperature of the reflected beam is determined by using Fig. 2 to give the X value corresponding to the phase angle of the reflected beam, and then utilizing Eq(17) to convert the X value to the temperature of the scattered molecules. In experiments where the beam was not heated, the last two terms of Eq(30) disappear.

RESULTS

Beam Temperature Variation

The phase shifts observed upon varying the temperature of the incident beam at constant surface temperature for a variety of gases on the annealed prism plane are shown in Table 1. The second column of this table gives the measured phase shifts which occur when the beam is heated to the temperatures indicated in the first column. The third column gives the calculated phase shifts due to decreased transit time from the chopper to the target, as determined from Fig. 2. This table shows that with the exception of neon and helium, the measured phase shifts

are equal to those calculated for the increase in the incident beam speed up to the target due to heating the molecular beam source.

Effect of Surface Temperature and the Solid Surface

The effect of the temperature of the solid on the temperature of the reflected beam was determined for all of the rare gases and several diatomic gases on the basal and prism planes of pyrolytic graphite. Both the as-received and annealed prism plane specimens were investigated. The beam temperature for most of these experiments was 300°K.

In Fig. 4, we have plotted the temperature of the reflected beam against the solid temperature for the rare gases on the annealed basal plane of graphite. Figs. 5 and 6 show the corresponding results for the prism plane in the annealed and as-received states. The data on these figures can be quite well represented by the empirical formula:

$$T_R/T_c = 1 - \exp(-T_s/T_c) \qquad (31)$$

where T_c is a constant which depends only upon the incident gas and the nature of the solid surface. A two-parameter fit to the data (i.e., allowing the T_c on the right hand side of Eq(31) to be different from the T_c on the left) did not provide a significantly better correlation.

The reflected temperatures determined from the annealed prism plane at beam temperatures greater than 300°K (Table 1)

are also shown on Fig. 5. Except for the oxygen point, the hot beam results fall on the same curves as the room temperature beam data.

The data when both the beam and the solid were at 300°K, of which the frequency scans shown in Fig. 3 represent a portion, are also shown in Figs. 4-6.

Table 2 summarizes the values of T_c for all the systems studied.

DISCUSSION

The experiments in which the temperature of the incident beam was varied from 300°K to 1300°K demonstrated that the mean speed of the reflected molecules is independent of the mean speed (or temperature) of the incident molecular beam - the consequences of the gas-solid interaction are unaffected by the state of the impinging gas molecule. This observation has several consequences:

First, the usual concept of a thermal accomodation coefficient defined by $(T_R-T_B)/(T_s-T_B)$, does not apply to these data, since the energy exchange process is not a function of beam temperature. The data of Table 1 reveal accomodation coefficients as defined above which are negative or greater than unity. However, global thermal accomodation coefficients could not be measured in the present study, since incidence and sampling angles were fixed.

Second, when the temperature of the beam and the solid are equal, the reflected beam temperature is generally less than either. For example, a xenon beam at 962°K impinging

on the solid at the same temperature is reflected at a temperature of ∿700°K.

Third, the only quantity which affects the temperature of the scattered gas is the temperature of the solid. T_R/T_s is always less than unity.

Fourth, these results cannot be explained by any of the current theories of thermal accomodation, which are dynamical in nature and consequently predict a close correlation between incident and reflected molecule energies. On graphite, the incident molecules are apparently trapped long enough to uncouple the re-emission process from the incident energy, but not long enough to attain complete thermal equilibrium with the solid. Analytical models of trapping on surfaces (18,19) are usually concerned with the trapping probability, which is easier to calculate than the desorption energy spectrum.

Weinberg and Merrill (20) have measured the trapping probability of rare gas atoms incident upon the tungsten (110) surface by determining the ratio of the diffusely scattered flux to the total scattered flux. They found that the trapping probabilities of argon, krypton and xenon were between 1/2 and 3/4, but that no helium or neon was trapped. In our experiments, the dependence of the scattered gas temperature upon incident beam temperature is a qualitative measure of the trapping probability. The energy of the desorbed molecules from the trapped portion of the incident beam should show no dependence upon the incident energy, whereas the energy of the

elastically scattered molecules should depend strongly upon incident energy. By this criterion, the trapping probabilities of the three heavy rare gases are unity. For helium and neon, however, the temperature of the scattered molecules did increase slightly with beam temperature, which indicates that not all of these gases were trapped on the surface prior to re-emission.

Weinberg and Merrill found that the trapping probability of argon, krypton and xenon decreased with increasing solid temperature. The present results for the same gases on graphite suggest that the trapping probabilities remain at unity for all solid temperatures. The energy of the desorbed atoms, however, is affected by solid temperature in a manner described by Eq(31).

According to Eq(31), the reflected beam cannot exceed the temperature T_c no matter how hot the solid is made. The observation of a critical or limiting temperature is in accord with the findings of Meyer and Gomer(9), although our T_c values are quite a bit larger than theirs. Moreover, we did not observe a discontinuous change in the nature of the energy exchange process as either the beam or solid temperature passed through the limiting temperature as did these authors.

Until a theory is developed to explain these results, T_c can only be regarded as an empirical parameter. However, it does have some of the attributes of a binding energy of the gas atoms to the solid. Fig. 7 shows that T_c increases in a regular manner as the atomic or molecular weight of the

gas increases. This behavior reflects the increasing well depth of the interaction potential with atomic weight. The critical temperature of deuterium is somewhat greater than that of helium, and that of oxygen is comparable to argon. The limiting temperature for hydrogen, however, is anomalously high.

Fig. 7 shows that the energy exchange process is the same on the basal and prism planes, as long as both have been annealed at high temperature prior to testing. Thermal accomodation on the as-received prism plane, however, is considerably more complete than on the annealed surfaces. The stronger interaction shown by the former is probably due to the greater roughness of this surface. On an atomic scale roughness increases the number of carbon atoms with which an impinging gas atom can strongly interact. Macroscopic roughness can assist thermal accomodation by providing more than a single collision of the incident atom with the solid. The difference between accomodation on two prism plane surfaces may be attributed to smoothing of the surface by the high temperature heat treatment.

Acknowledgment

This work was carried out under the auspices of the United States Atomic Energy Commission.

TABLE 1. RESULTS OF THE BEAM HEATING EXPERIMENTS - ANNEALED PRISM PLANE PYROLYTIC GRAPHITE

Incident Beam Temp., °K	$\Delta\phi_{(\text{beam heat})}$, deg	$[\phi_f(300) - \phi_f(T_B)]$ deg[a]	Reflected Beam Temp., °K
xenon; $\phi_d(300)=93°$; $T_s=300°K$; $\Delta\phi_{(\text{target heat})}=0$			
423	8.7	9.8	302
645	16.3	19.6	288
881	22.0	25.7	285
1098	25.4	29.8	299
1250	26.7	31.7	276
		average =	290±8
xenon; $\phi_d(300)=93°$; $T_s=962°K$; $\Delta\phi_{(\text{target heat})}=28.8°$			
406	9.1	8.6	746
576	15.6	17.0	697
600	16.4	18.0	697
818	22.6	24.2	697
1077	26.8	29.5	668
1284	29.0	32.2	658
		average =	694±21

[a] from Fig 2.

Incident Beam Temp., °K	$\Delta\phi_{(\text{beam heat})}$, deg	$[\phi_f(300) - \phi_f(T_B)]$ deg	Reflected Beam Temp., °K
krypton; $\phi_d(300)=78.5°$; $T_s=1003°K$; $\Delta\phi_{(\text{target heat})}=22.2°$			
401	6.7	7.0	622
568	12.3	14.0	585
688	16.2	17.4	597
916	20.7	21.8	597
1105	23.0	24.6	588
1258	24.6	26.5	579
		average =	595±11
neon; $\phi_d(300)=41°$; $T_s=428°K$; $\Delta\phi_{(\text{target heat})}=3.6°$			
421	5.2	4.3	257
564	8.7	7.3	266
765	12.0	9.8	277
973	14.2	11.8	281
1248	16.3	13.8	282
		average =	273±9
neon; $\phi_d(300)=41°$; $T_s=987°K$; $\Delta\phi_{(\text{target heat})}=8.5°$			
407	3.9	3.8	491
575	8.0	7.5	510
758	11.3	9.8	551
973	13.5	11.8	530
1249	15.1	13.6	551
		average =	527±21

Incident Beam Temp., °K	$\Delta\phi_{(\text{beam heat})}$, deg	$[\phi_f(300) - \phi_f(T_B)]$ deg	Reflected Beam Temp., °K
oxygen; $\phi_d(300)=51°$; $T_s=979°K$; $\Delta\phi_{(\text{target heat})}=12.1°$			
421	4.9	5.4	522
564	8.5	9.2	522
868	12.9	13.9	522
1077	15.1	15.7	522
1265	16.4	17.1	522
			average = 522±0
helium; $\phi_d(300)=19°$; $T_s=977°K$, $\Delta\phi_{(\text{target heat})}=2.8°$			
542	4.1	3.0	460
761	5.3	4.2	460
944	6.8	5.0	512
1256	7.5	5.9	499
			average = 483±23
helium; $\phi_d(300)=19°$; $T_s=751°K$; $\Delta\phi_{(\text{target heat})}=2.8°$			
393	2.0	1.4	441
395	2.1	1.4	441
585	4.3	3.3	441
814	5.9	4.5	486
1042	6.9	5.3	499
1235	7.6	5.8	508
			average = 469±28

Incident Beam Temp., °K	$\Delta\phi_{(\text{beam heat})}$, deg	$[\phi_f(300) - \phi_f(T_B)]$ deg	Reflected Beam Temp., °K
helium; $\phi_d(300)=19°$; $T_s=921°K$; $\Delta\phi_{(\text{target heat})}=3.0°$			
394	2.1	1.4	441
591	4.5	3.2	490
932	6.5	5.0	503
1241	7.7	5.8	526
			average = 490±25
deuterium; $\phi_d(300)=19°$; $T_s=873°K$; $\Delta\phi_{(\text{target heat})}=3.7°$			
351	1.7	0.8	508
591	3.3	3.4	441
818	4.9	4.5	478
993	5.6	5.2	478
1260	6.4	5.8	482
			average = 477±15
deuterium; $\phi_d(300)=19°$; $T_s=960°K$; $\Delta\phi_{(\text{target heat})}=0.6°$			
411	1.9	1.7	323
683	4.3	4.0	325
1016	5.1	5.3	316
1266	5.7	6.0	306
			average = 318±7

TABLE 2. LIMITING TEMPERATURES OF GASES REFLECTED FROM VARIOUS SURFACES OF PYROLYTIC GRAPHITE

Gas	T_c, °K		
	As-Received Prism Plane	Annealed Prism Plane	Annealed Basal Plane
H_2	1113	---	---
D_2	722	---	---
He	614	---	602
Ne	903	615	---
O_2	1027	861	---
Ar	1260	---	752
Kr	2637	902	981
Xe	3710,3407[a]	1274	1026

[a]The two values of T_c represent two independent experiments. No distinction is made between the points from the two experiments in the upper curve of Fig. 6.

REFERENCES

1. A.F. Devonshire, Proc. Royal Soc. (London) A158 (1937) 269.

2. C. Strachan, Proc. Royal Soc. (London) A158 (1937) 591.

3. N. Cabrera, Trans. Faraday Soc. 28 (1959) 16.

4. F.W. Zwanzig, J. Chem. Phys. 32 (1960) 1173.

5. F.O. Goodman, J. Phys. Chem. Solids 23 (1962) 1269; Surface Science 7 (1967) 391; Surface Science 11 (1968) 283; J. Chem. Physics 50 (1969) 3855.

6. L. Trilling, Surface Science 27 (1971).

7. L.B. Thomas in Rarefied Gas Dynamics, 5th Symp., Vol. 1 (Academic Press, New York, 1967) pp. 155-162; J. Kouptsidis and D. Menzel, Bunsenges. 74 (1970) 512.

8. R.E. Forman, J. Chem. Phys. 55, 2839 (1971).

9. L. Meyer and R. Gomer, J. Chem. Phys. 28, 617 (1958).

10. D.R. Olander, W.J. Siekhaus, R.H. Jones, and J.A. Schwarz, J. Chem. Phys. (to be published).

11. G.S. Holister, R.T. Brackmann and W.L. Fite, Planetary and Space Science 3, 162 (1961).

12. S. Yamamoto and R.E. Stickney, J. Chem. Phys. 53, 1594 (1970).

13. R.H. Jones, D.R. Olander, W.J. Siekhaus, and J.A. Schwarz, J. Vac. Sci. Technol., (to be published).

14. The scattering probability is a function of incident and reflected angles as well as of molecular speeds (E.P. Wenaas, J. Chem. Phys., 54, 376 (1971)). In general, $p(v',\theta',v,\theta)dvd\Omega$ is the probability that a molecule of speed v' incident upon the surface at polar angle θ' is reflected into the solid angle $d\Omega$ about θ with a speed in the range from v to v+dv. If $\Delta\Omega$ is the solid angle subtended by the

detector opening from the target, the quantity P_θ is:

$$P_\theta = \int_0^\infty dv \int_{\Delta\Omega} p(v'\theta', v, \theta) d\Omega$$

and the speed distribution function of those molecules scattered into $\Delta\Omega$ is:

$$p(v', v) = \frac{1}{P_\theta} \int_{\Delta\Omega} p(v', \theta', v, \theta) d\Omega$$

for simplicity of notation, the angular variables have been omitted since they were not varied in the experiments.

15. H. Harrison, D.G. Hummer, and W.L. Fite, J. Chem. Phys 41, 2567 (1964).

16. S. Yamamoto and R.E. Stickney, J. Chem. Phys. 47, 1091 (1967).

17. Molecular beams generated by multichannel sources may have speed distributions somewhat harder than a Maxwellian spectrum at the beam source temperature (W.J. Siekhaus, R.H. Jones and D.R. Olander, J. Appl. Phys. 41, 4392 (1970)). In the worst case, the average energy is 5.5% greater than that of a Maxwellian beam at the same temperature, but the shape of the distribution function is similar to that of a Maxwellian Spectrum. This distortion reduces the chopper-to-surface phase shift by about 3° for xenon at 1500 Hz. The effect is not significant.

18. W.H. Weinberg and R.P. Merrill, J. Vac. Sci. Technol. (to be published).

19. J.L. Beeby and L. Pobrzynski, J. Phys. C: Solid St. Phys. 4, 1269 (1971).

20. W.H. Weinberg and R.P. Merrill, J. Chem. Phys. 56, 2881 (1972).

LIST OF FIGURES

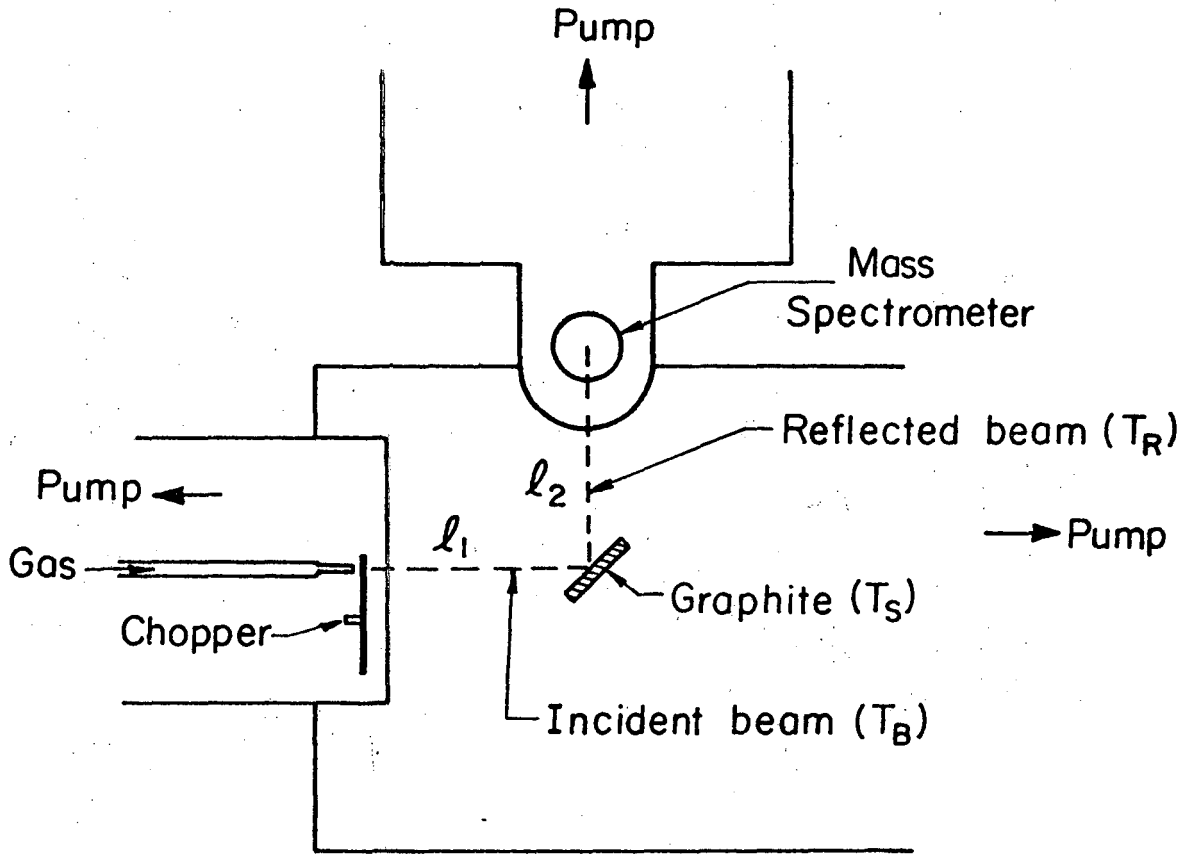

XBL 722-6038

Fig. 1

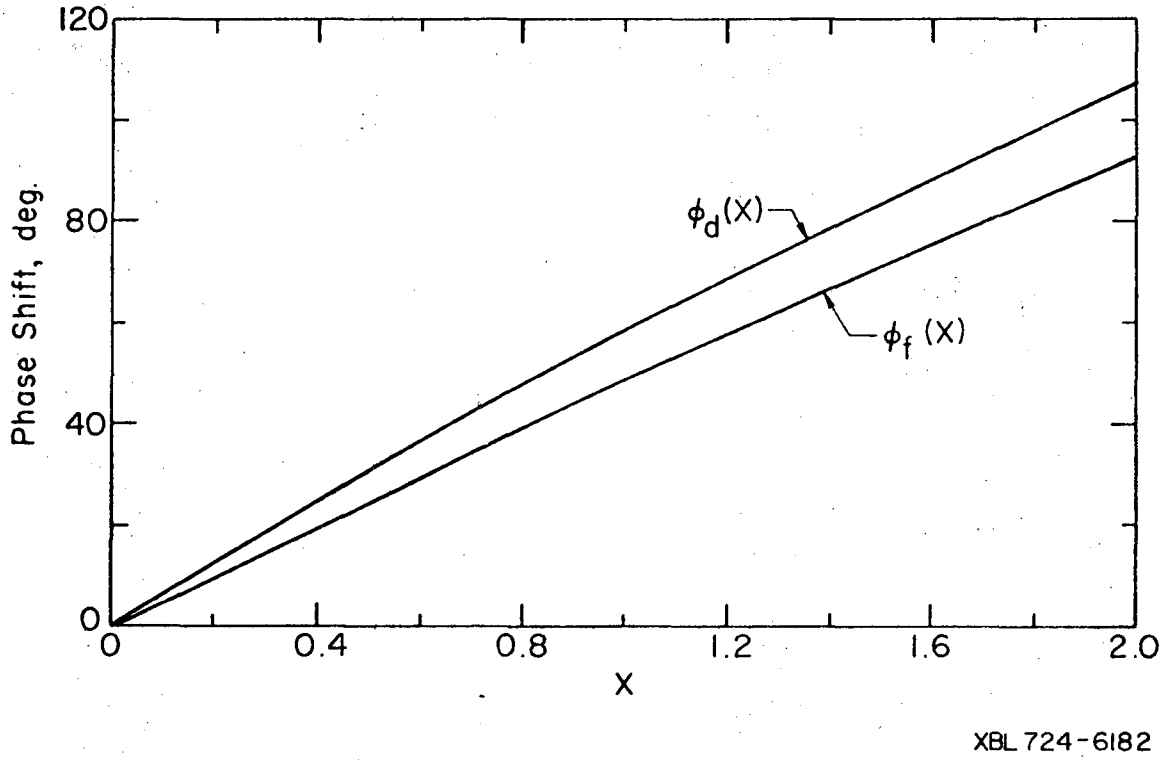

XBL 724-6182

Fig. 2

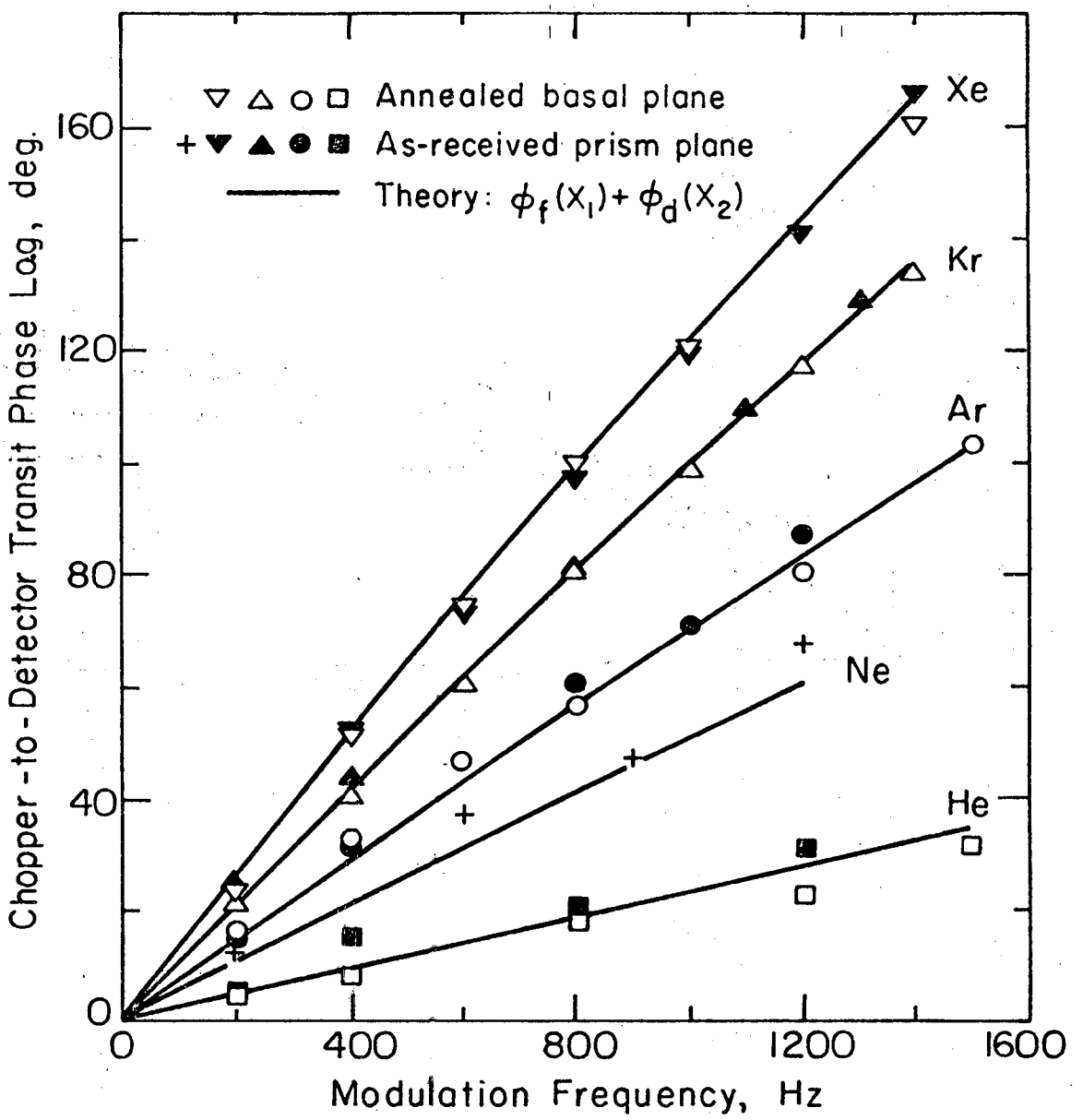
Annealed basal plane
As-received prism plane
Theory: $\phi_f(X_1)+\phi_d(X_2)$
Xe
Kr
Ar
Ne
He
Chopper-to-Detector Transit Phase Lag, deg.
0
40
80
120
160
0
400
800
1200
1600
Modulation Frequency, Hz
XBL724-6183

Fig. 3

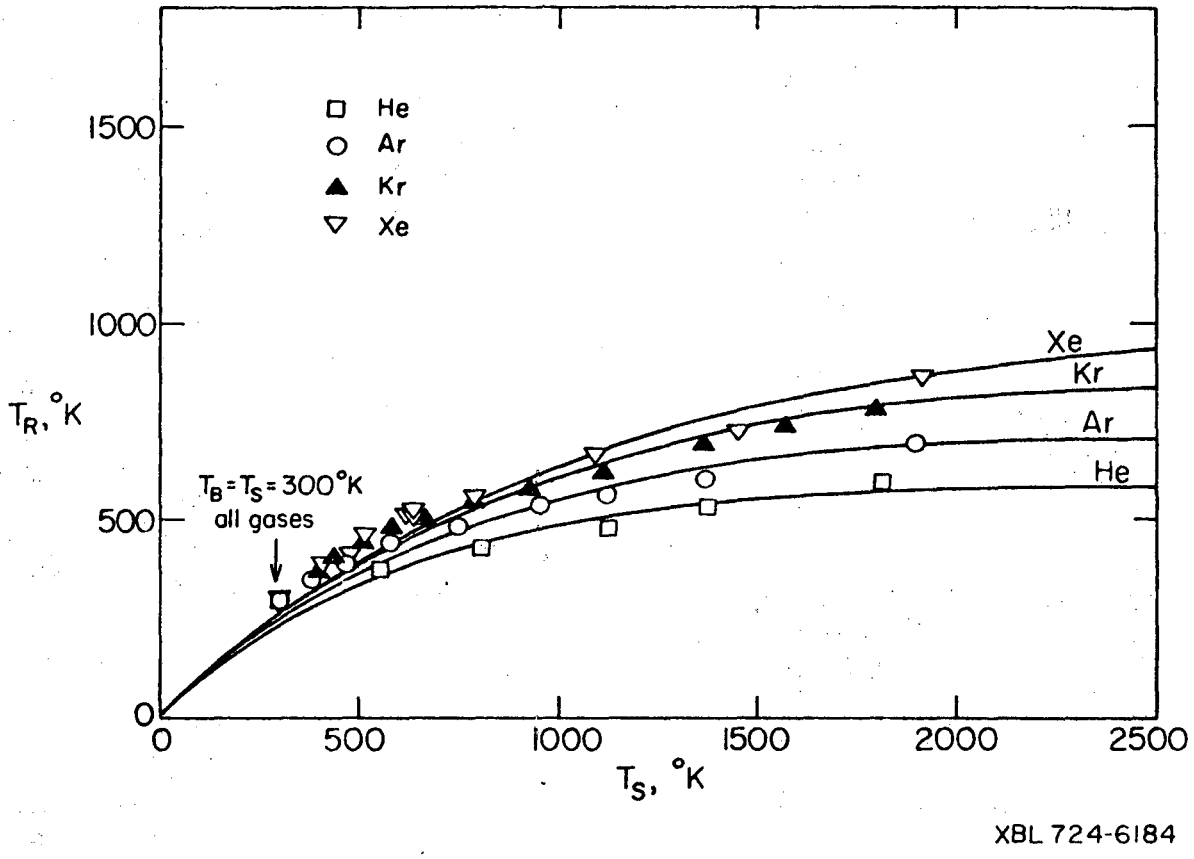
He
Ar
Kr
Xe
1500
1000
500
0
T_R, °K
$T_B = T_S = 300$°K
all gases
Xe
Kr
Ar
He
0
500
1000
1500
2000
2500
T_S, °K
XBL 724-6184

Fig. 4

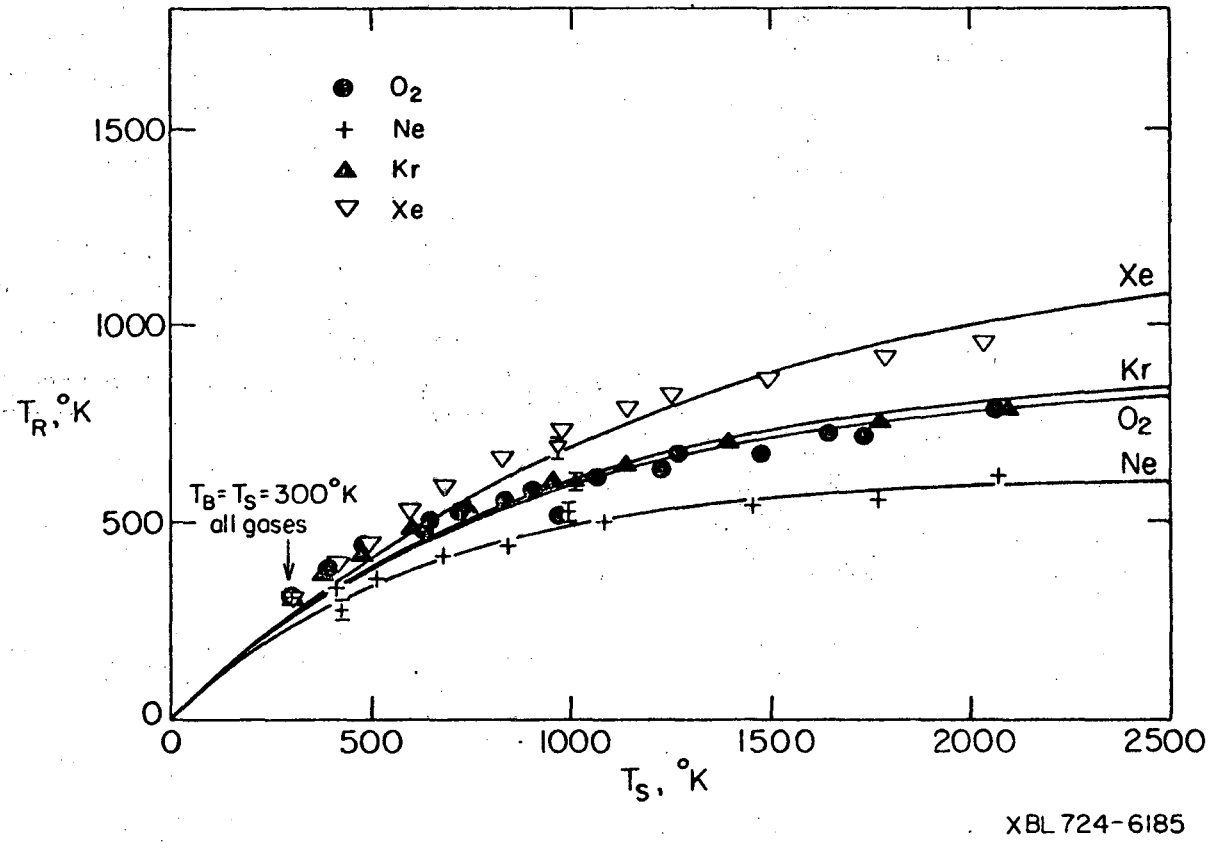
O2
Ne
Kr
Xe
1500
1000
500
0
TR, °K
TB = TS = 300°K
all gases
Xe
Kr
O2
Ne
0
500
1000
1500
2000
2500
TS, °K
XBL 724-6185

Fig. 5

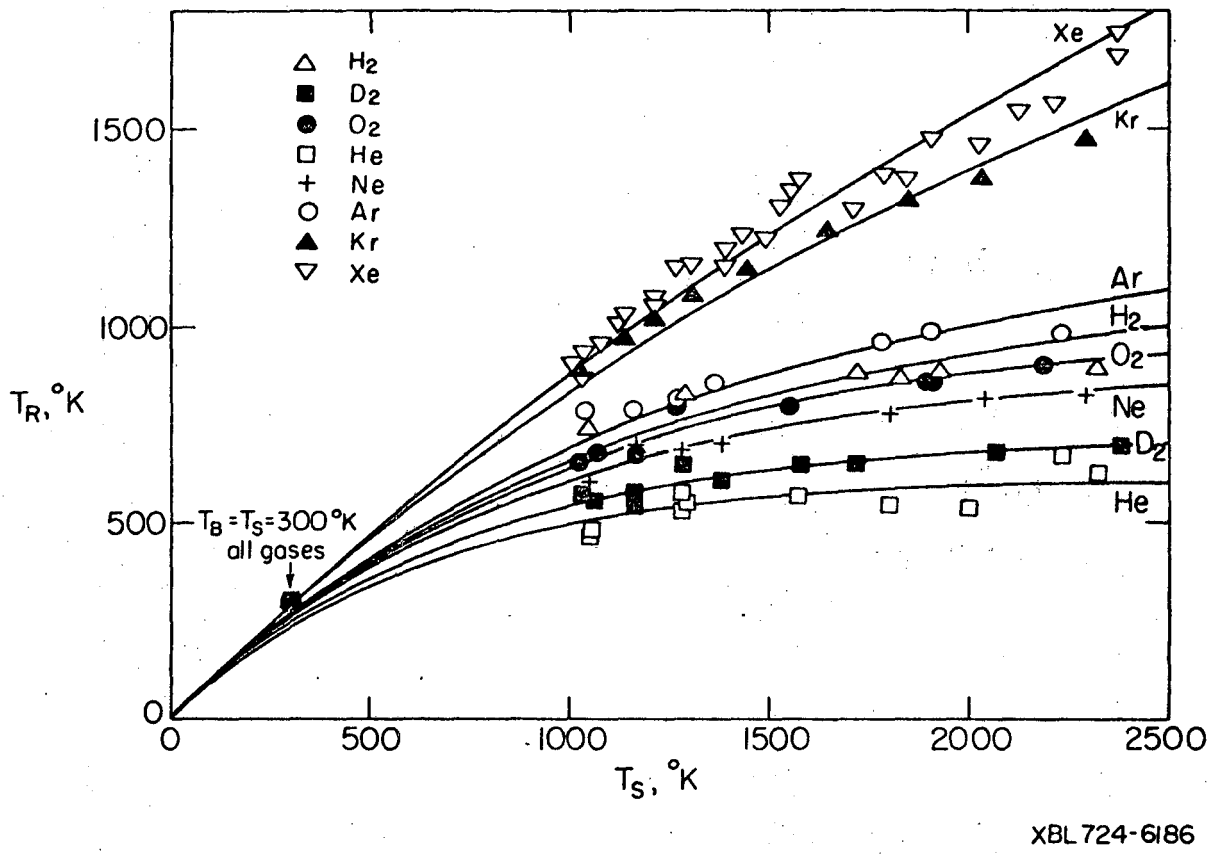
H2
D2
O2
He
Ne
Ar
Kr
Xe
1500
1000
500
0
TR, °K
TB = TS = 300 °K
all gases
0
500
1000
1500
2000
2500
TS, °K
Xe
Kr
Ar
H2
O2
Ne
D2
He
XBL 724-6186

Fig. 6

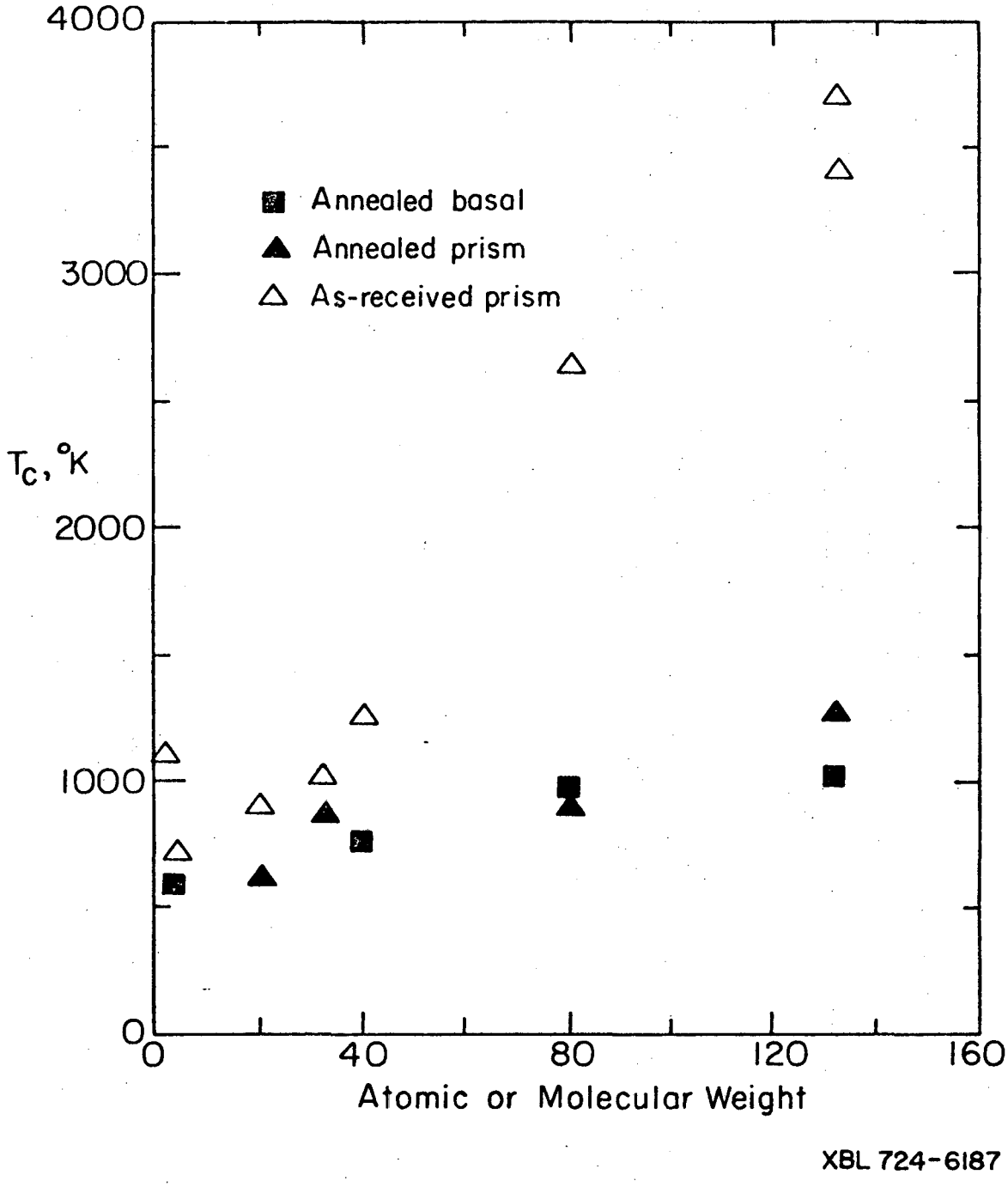
4000
3000
2000
1000
0
T_c, °K
Annealed basal
Annealed prism
As-received prism
0
40
80
120
160
Atomic or Molecular Weight
XBL 724-6187

Fig. 7

TECHNICAL INFORMATION DIVISION
LAWRENCE BERKELEY LABORATORY
UNIVERSITY OF CALIFORNIA
BERKELEY, CALIFORNIA 94720